LAWRENCE
LIVERMORE
NATIONAL
LABORATORY

LLNL-CONF-481131

Low and High Temperature Combustion Chemistry of Butanol Isomers in Premixed Flames and Autoignition Systems

S. M. Sarathy, W. J. Pitz, C. K. Westbrook, M. Mehl, K. Yasunaga, H. J. Curran, T. Tsujimura, P. Osswald, K. Kohse-Hoinghaus

April 25, 2011

Combustin Institute US Meeting 2011
Atlanta, GA, United States
March 20, 2011 through March 24, 2011

Disclaimer

This document was prepared as an account of work sponsored by an agency of the United States government. Neither the United States government nor Lawrence Livermore National Security, LLC, nor any of their employees makes any warranty, expressed or implied, or assumes any legal liability or responsibility for the accuracy, completeness, or usefulness of any information, apparatus, product, or process disclosed, or represents that its use would not infringe privately owned rights. Reference herein to any specific commercial product, process, or service by trade name, trademark, manufacturer, or otherwise does not necessarily constitute or imply its endorsement, recommendation, or favoring by the United States government or Lawrence Livermore National Security, LLC. The views and opinions of authors expressed herein do not necessarily state or reflect those of the United States government or Lawrence Livermore National Security, LLC, and shall not be used for advertising or product endorsement purposes.

7th US National Technical Meeting
of the Combustion Institute
Hosted by the Georgia Institute of Technology, Atlanta, GA
March 20-23, 2011

Low and High Temperature Combustion Chemistry of Butanol Isomers in Premixed Flames and Autoignition Systems

S.M. Sarathy[1*], K. Yasunaga[2], S. Vranckx[3], P. Oßwald[4]
C. K. Westbrook[1], M. Mehl[1], W.J. Pitz[1], H.J. Curran[2], T. Tsujimura[5], K. Kohse-Hoinghaus[4], R.X. Fernandez[3]

[1] *Lawrence Livermore National Laboratory, Livermore, California, USA*
[2] *National University of Ireland, Galway, Ireland*
[3] *RWTH Aachen University, Germany*
[4] *Bielefeld University, Bielefeld, Germany*
[5] *National Institute of Advanced Industrial Science and Technology, Tsukuba, Ibaraki, Japan*

**** Corresponding author***
sarathy1@llnl.gov
925.423.6011

Butanol is a fuel that has been proposed as a bio-derived alternative to conventional petroleum derived fuels. The structural isomer in traditional "bio-butanol" fuel is n-butanol, but newer conversion technologies produce iso-butanol as a fuel. In order to better understand the combustion chemistry of bio-butanol, this study presents a comprehensive chemical kinetic model for all the four isomers of butanol (e.g., *1*-, *2*-, *iso*- and *tert*-butanol). The proposed model includes detailed high temperature and low temperature reaction pathways. In this study, the primary experimental validation target for the model is premixed flat low-pressure flame species profiles obtained using molecular beam mass spectrometry (MBMS). The model is also validated against previously published data for premixed flame velocity and *n*-butanol rapid compression machine and shock tube ignition delay. The agreement with these data sets is reasonably good. The dominant reaction pathways at the various pressures and temperatures studied are elucidated. At low temperature conditions, we found that the reaction of alphahydroxybutyl with O_2 was important in controlling the reactivity of the system, and for correctly predicting C_4 aldehyde profiles in low pressure premixed flames. Enol-keto isomerization reactions assisted by HO_2 were also found to be important in converting enols to aldehydes and ketones in the low pressure premixed flames.. In the paper, we describe how the structural features of the four different butanol isomers lead to differences in the combustion properties of each isomer.

1.0 Introduction

The goal of this study is to develop a new chemical kinetic model for the four isomers of butanol: *1*-butanol, *2*-butanol, *iso*-butanol, and *tert*-butanol. This study differentiates itself from the previous butanol isomers chemical kinetic model [1] by including detailed high and low temperature pathways with reaction rate constants based extensively on *ab initio* rate calculations. There have many previous combustion studies on the various butanol isomers, and reviewing them is beyond the scope of the present paper. The primary focus is to present a new model of all four isomers that includes both high temperature and low temperature reaction pathways. The model is widely validated against recently published experimental data from low-pressure premixed flames [2]. It is also further validated against data for premixed flame velocities [3-5] and *n*-butanol rapid compression machine [7] and shock tube [8,9] ignition delay times.

2.0 Chemical Kinetic Model Development

The chemical kinetic model is an improvement on previously developed models from NUI Galway [6], LLNL [4], and the RWTH Aachen University [9]. We started with the *1*-butanol mechanism developed by Black et al [6]. This mechanism was expanded by adding primary reactions of *tert*-, *2*-, and *iso*-butanol and related radicals reactions to the *1*-butanol reaction mechanism. The following is a list of specific additions:

- The H atom abstraction rates by OH radicals from the alpha and beta carbons were updated based on the calculations by Zhou et al. [10]. The abstraction rates for sites more than two carbons away from the hydroxyl group (e.g., gamma and delta carbon atoms in *1*-butanol) were taken to be analogous to abstraction rates from an *1*-alkane [11].
- The H atom abstraction rates by radicals H and CH_3 from the alpha and beta carbons were updated based on the calculations by Carstensen and Dean [12], which quantify the effects of the hydroxyl moiety. The abstraction rates for sites more than two carbons away from the hydroxyl group (e.g., gamma and delta carbon atoms in *1*-butanol) were taken to be analogous to abstraction rates from an *1*-alkane [11].
- Reactions of enols + HO_2 <=> aldehyde + HO_2 were added to the mechanism based on the work of da Silva and Bozzelli [13]. These reactions are faster paths of enol-keto isomerization.
- Radical isomerization rates for butoxyl radicals were included based on the work of Zheng and Truhlar [15].
- The alphahydroxyethyl (i.e., sc2h4oh) chemistry from Simmie and Curran [16] was added.
- Reactions of alphahydroxybutyl plus O_2 forming butyraldehyde + HO_2 were updated based on the work of da Silva and Bozzelli [17] on alphahydroxyethyl radicals. We selected the calculated high pressure limit rate constant.
  e.g. $C_4H_8OH\text{-}1 + O_2 <=> nC_3H_7CHO + HO_2$
- Several changes were made to the C_2H_5 and C_2H_3 chemistry to improve agreement in low-pressure flame systems. The new reaction rates are pressure dependent values based on the work of Senosiain et al. [18].
- Low temperature pressure dependent reaction pathways for *1*-butanol were added from the work of Vranckx et al. [9].
- Detailed enol chemistry was added from the work of Veloo et al. [4]

3.0 Results and Discussion

3.1 Low pressure flat flame simulations

All simulations were conducted in CHEMKIN PRO using the fuel flow rates and burner dimensions provided in Oßwald et al. [2]. The experimentally measured temperature profiles were used to solve the flame simulation. The original temperatures presented in Oßwald et al. [2] were from an unperturbed flame, and these provided poor results when inserted into the model. It was determined that the temperatures are regions near to the burner port were too hot, and thus the fuel was being consumed too rapidly. In order to better reproduce the data obtained from the flame perturbed by the sampling cone, the temperature profile was calculated based on the MBMS-data (i.e., using transfer function [19]). The resulting temperature profiles provided much better results when inserted in the simulation. Nevertheless, the simulated results were additionally shifted 1 mm away from the burner port to provide better agreement with the experimental data.

The following sections present figures of the simulations compared with the experimental data from Oßwald et al. [2]. The graphs have been prepared in a similar format to the original paper, wherein a product's distribution is presented for all four isomers on the

same figure. In the discussion, we consider predictions within a factor of 2-2.5 of the experimental data to be good.

The major species profiles for the each butanol isomer includes measurements for the fuel, Ar, CO, CO_2, H_2O, H_2, and O_2. The model predictions for all major species are excellent, and we provide figures of these comparisons as supplementary material. Experimental data is shown for measurements taken using electron impact ionization (EI) and photo ionization (PI) techniques discussed in [2].

3.2 C_4H_8O species (butanal and/or butanones)

The experimental results indicated that negligible amounts of butenol species were found in all the flames, so the C_4H_8O isomers measured are primarily butanals and butanones. It was originally thought that these C_4H_8O species were formed after H abstraction from the alpha carbon and then beta-scission to lose an H atom. However, *ab initio* calculations [16] suggest that such reactions are too slow to be significant, and a model consisting of only H atom abstraction and beta-scission reactions under predicts the experimental data.

The model presented here improves the prediction of C_4H_8O products by including alternate pathways to form these compounds. The compounds are actually formed after H atom abstraction from the alpha carbon followed by O_2 addition to the radical site. An adduct is formed, which eventually eliminates HO_2 to produce C_4H_8O (e.g., C_4H_8OH-1 + O_2<=>nC_3H_7CHO + HO_2). Similar reactions are known to be important for ethanol in low temperature oxygen rich systems [17].

In Figure 1 the model well predicts C_4H_8O concentrations for *1*-butanol, *2*-butanol, and *iso*-butanol. Both the simulations and the measurements show C_4H_8O formation is much less important in the tert-butanol flame. However, the model predicts no C_4H_8O formation because there is no alpha site for H atom abstraction in *tert*-butanol. So the channel of O_2 addition to the alphahydroxybutyl site does not exist for *tert*-butanol. Thus, we are unable to explain the small butanone formation in the *tert*-butanol flame.

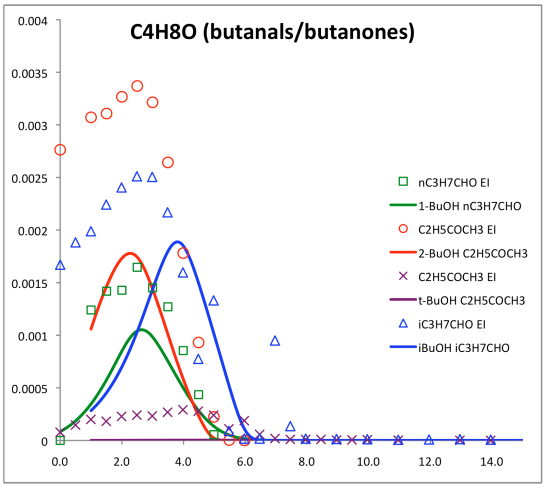

Figure 1 - Experimental and predicted profiles for C_3H_6O species butanal/butanones.

3.3 C_3H_6O species

The isomers of C_3H_6O measured in the flames include *1*-propenol ($CH_3CHCHOH$), *iso*-propenol (iC_3H_5OH), acetone+allyl alcohol, and propanal (C_2H_5CHO). The concentrations of acetone and allyl alcohol (CH_2CHCH_2OH) are combined in the simulation because the species measurements are indistinguishable due to similar ionization thresholds in the mass spectrometer.

3.3.1 1-propeno/iso-propenol

The predictions of *1*-propenol/*iso*-propenol are shown in Figure 2. These species are presented together because they are inseparable due to similar ionization thresholds. The *1*-butanol flame does not produce much *1*-propenol ($CH_3CHCHOH$), which is in agreement with the model. The *2*-butanol model predicts correct amounts of *iso*-propenol, which is formed by H atom abstraction from the alpha carbon followed by beta scission leading to CH_3 and iC_3H_5OH. The iC_3H_5OHcould tautomerize to acetone, but these unimolecular reactions are slow in the gas phase. The model includes alternate pathways of enol-keto isomerization via reactions with HO_2 [13], which are active in the model and responsible for consuming iC_3H_5OH.

The model overpredicts *1*-propenol in the *iso*-butanol flame and *iso*-propenol in the *tert*-butanol flame. The model predicts that *1*-propenol is formed in the *iso*-butanol flame by H atom abstraction from the alpha carbon followed by beta scission leading to CH_3 and *1*-propenol. The *tert*-butanol flame produces *iso*-propenol by H atom abstraction from any of the beta carbons and beta scission leading to CH_3 + *iso*-propenol. The aforementioned reaction pathways predicted by the model are expected, so we are unable to rationalize the over predictions by the model at this time.

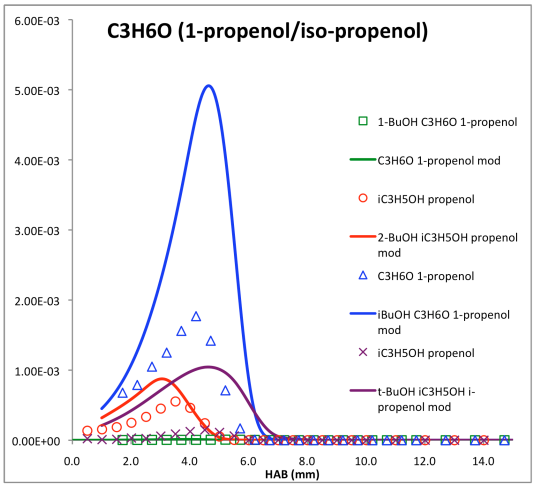

Figure 2 - Experimental and predicted profiles for C_3H_6O species *1*-propenol/*iso*-propenol.

3.3.2 Acetone/allyl alcohol

Acetone and allyl alcohol (CH_2CHCH_2OH) are indistinguishable due to similar ionization thresholds, so the model's predictions of these species is combined in Figure 3. The *1*-butanol model and experiments both show little acetone + allyl alcohol being formed. The model predicts that the primary contribution is from allyl alcohol, which is formed by H atom abstraction from the beta carbon and subsequent beta scission forming CH_3 and allyl alcohol.

The *2*-butanol flame data shows appreciable levels of acetone + allyl alcohol and the model underpredicts the concentration. The model predicts that the primary contribution is from acetone, which is formed from *iso*-propenol (shown previously) via HO_2 assisted enol-keto isomerization (e.g., $iC_3H_5OH + HO_2 = CH_3COCH_3 + HO_2$). For *2*-butanol flame, the model predicts *iso*-propenol concentration to be similar to the acetone concentration, while the experimental data shows nearly ten times greater concentration of acetone versus *iso*-propenol.

For the *iso*-butanol flame, the model over predicts the concentration of acetone + allyl alcohol. The majority of this predicted concentration is from allyl alcohol, which is formed by H atom abstraction from the primary (i.e., gamma) carbon and subsequent beta scission forming CH_3 and allyl alcohol. We are unable to explain why the experiments do not show the presence of allyl alcohol.

For *tert*-butanol, the experimental data shows the presence of appreciable levels of acetone + allyl alcohol. The model predicts the major species to be acetone, which is formed from *iso*-propenol via HO_2 assisted enol-keto isomerization. The model includes a pathway to acetone via unimolecular decomposition leading to CH_3 and acetone; however, this reaction is very slow at the lower temperatures in the flame where the acetone concentration reaches a maximum. The over prediction of *iso*-propenol and under prediction of acetone suggests that the rate HO_2 assisted enol-keto isomerisation may be faster than currently estimated.

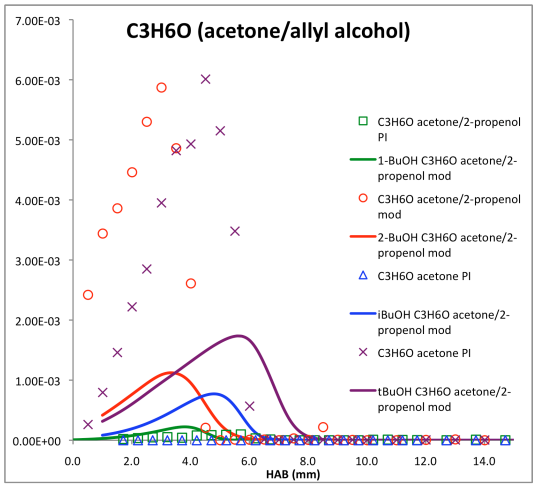

Figure 3 - Experimental and predicted profiles for C_3H_6O species acetone+allyl alcohol.

3.3.3 Propanal

Propanal was found to be negligible in both experiments and simulations of *2*-butanol and *tert*-butanol flames. In Figure 4, the model well predicts the concentrations of propanal in the *1*-butanol and *iso*-butanol flames. In the *1*-butanol model, propanal is formed in small quantities from recombination of the radicals CH_3 and CH_2CHO. The *iso*-butanol model predicts that propanal is formed from 1-propenol via HO_2 assisted enol-keto isomerization.

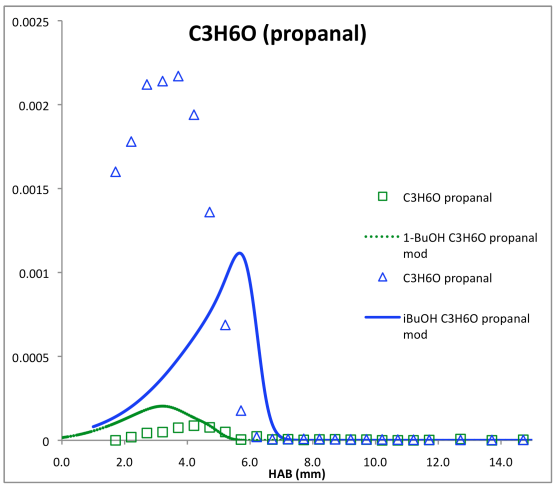

Figure 4 - Experimental and predicted profiles for C_3H_6O species propanal.

3.3.4 Ethenol and Acetladehyde

The flame experiments are capable of differentiating the C_2H_4O isomers ethanol and acetaldehyde. In Figure 5, the agreement between model and experiments is good for the *iso*-butanol, *2*-butanol, and *tert*-butanol systems. The *1*-butanol model predicts more ethanol than acetaldehyde, while the experimental data shows the reverse trend. The model predicts ethenol is formed in higher concentrations by H atom abstraction from the alpha carbon followed by beta scission to CH_3 plus ethenol. The acetaldehyde is formed from ethenol via HO_2 assisted enol-keto isomerization.

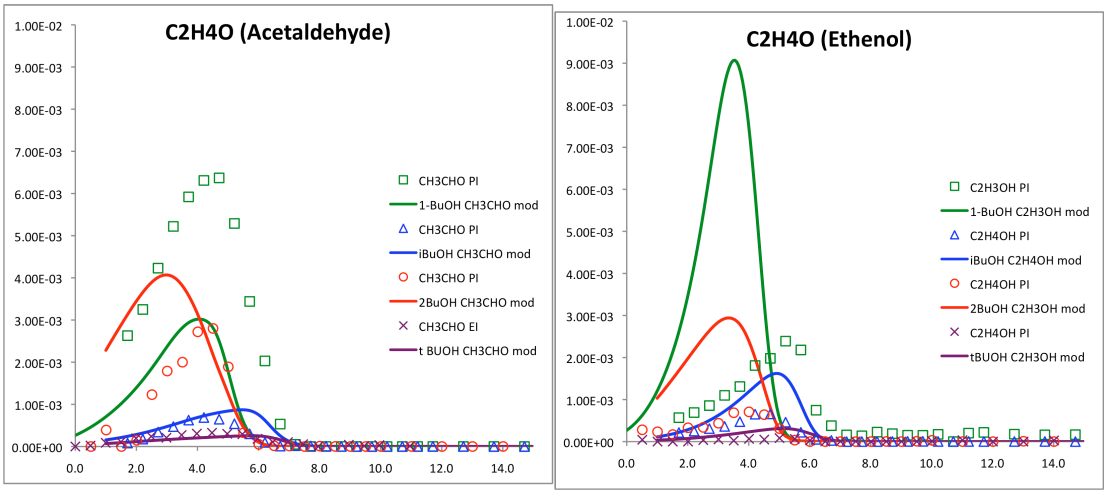

Figure 5 - Experimental and predicted profiles for C_2H_4O species acetaldehyde and ethenol.

3.3.5 Formaldehyde and Ketene

The formaldehyde and ketene concentrations measured in the experiments are generally well predicted by the model for all four isomers, as shown in Figure 6.

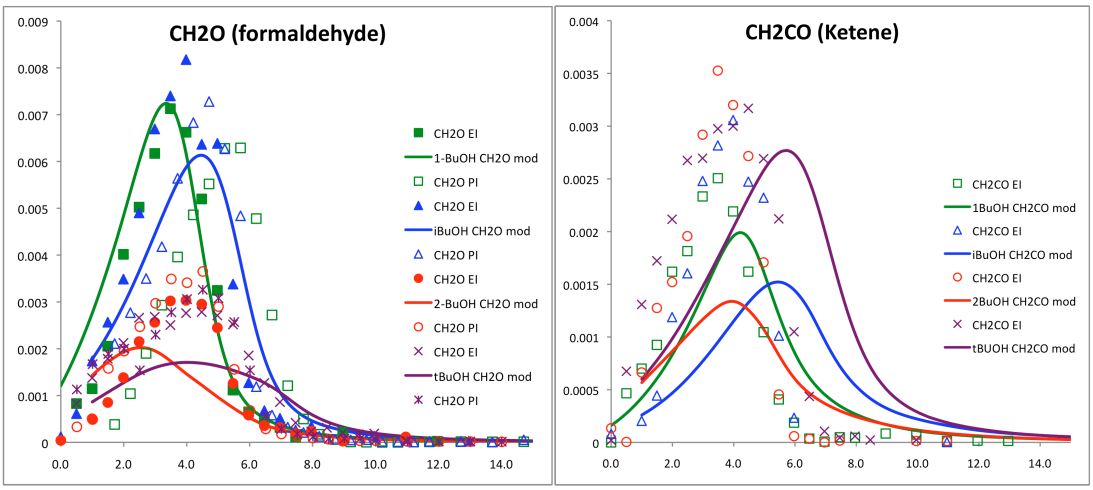

Figure 6 - Experimental and predicted profiles for formaldehyde (CH_2O) and ketene (CH_2CO).

3.3.6 Butene isomers

The isomers of butene (C_4H_8) include *1*-butene, *2*-butene, and *iso*-butene. The experiments are unable to differentiate these species, but it is easy to predict the structure based on the fuel. In Figure 7, the models for the four isomers of butanol do a reasonable job of predicting the experimental C_4H_8 profiles. *1*-Butanol is shown to produce *1*-butene by H atom abstraction from the beta carbon followed by beta scission to OH and 1-C_4H_8. Similarly the other isomers all undergo H atom abstraction from the beta carbon and then beta scission to lose the OH group and form either *2*-butene or *iso*-butene. It should be noted that butenes could also be formed by unimolecular elimination of H_2O; these reactions are included in the model but the high activation energies make them unimportant in these premixed flames where H atom abstraction reactions are predominant.

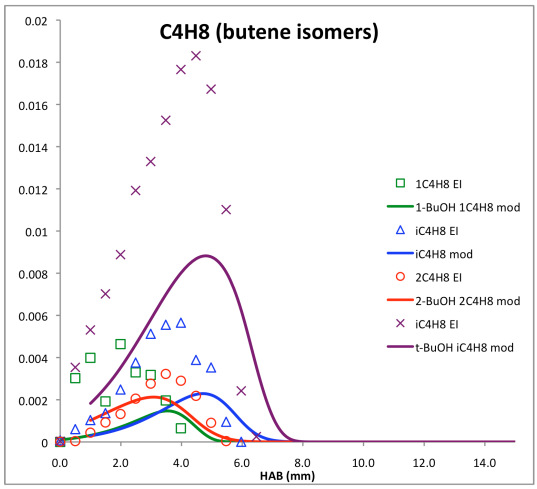

Figure 7 - Experimental and predicted profiles for C_4H_8 species *1*-butene, *2*-butene, and *iso*-butene.

3.3.7 C1, C2, and C3 species

The remaining graphs in Figure 8 on the page show experimental and modeling data for C_1, C_2 and C_3 species. The model shows reasonably good agreement for CH_3, CH_4, C_2H_4, C_2H_6, aC_3H_4, (allene), C_3H_8, C_3H_6, C_2H_5, and HCO. pC_3H_4 (propyne) is under predicted by the model, which suggests there may be some pathways missing in the model.

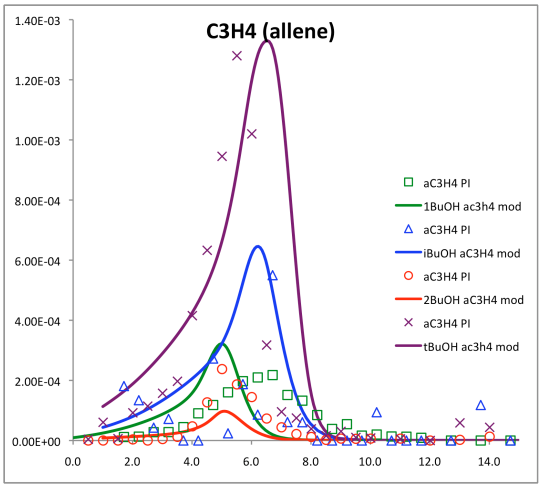

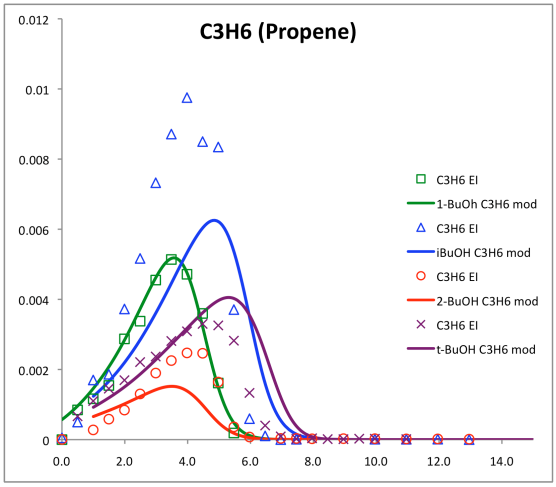

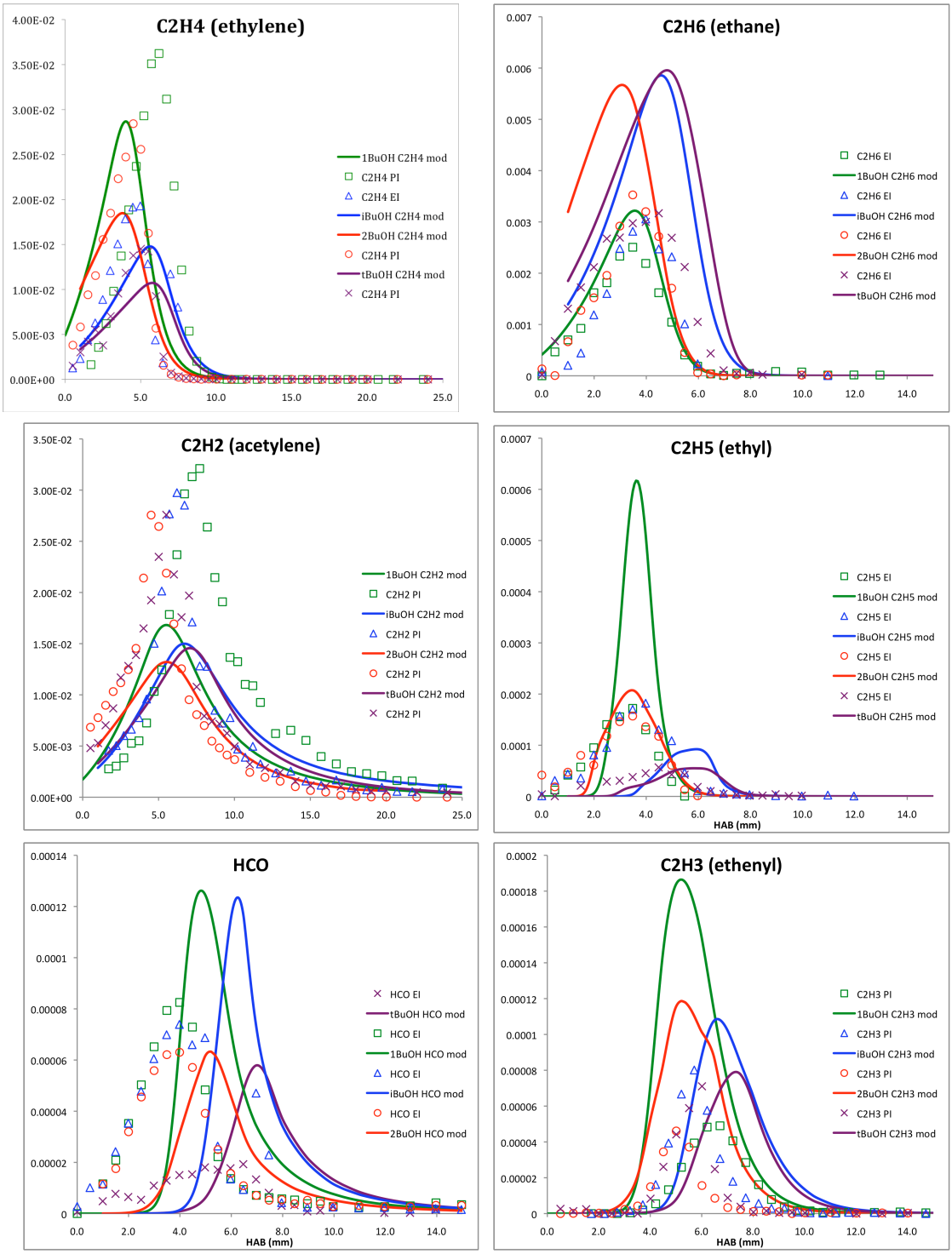

Figure 8 - Experimental and predicted profiles for C_2 ad C_3 species.

3.3.8 Other C_3, C_4, C_5, C_6, and C_8 species

The other C_4 species measured in the experiments included C_4H_6 (*1*-butyne and *2*-butyne), C_4H_5, C_4H_4, C_4H_3, 1,3-C_4H_6 (1,3-butadiene), and C_4H_2. At this stage the model is unable to accurately predict these species because the base C_4 chemistry does not include recombination reactions leading to highly unsaturated C_4 and larger hydrocarbons. For the same reasons, pC_3H_4 (propyne), C_3H_5, C_3H_3, C_6H_6, C_5H_6, and C_8H_6 were all measured in the experimental flames but not predicted well by the model.

3.4 Premixed Laminar Flame Velocity Simulations

Premixed laminar flame velocities (S_u^0) have been reported for *1*-butanol [3,4,5], *iso*-butanol [3,5], *2*-butanol [3], and *tert*-butanol [3]. S_u^0 was modelled using the PREMIX flame code in CHEMKIN PRO. Simulations were conducted assuming mixture-averaged transport, and accounting for thermal diffusion. The converged solutions had approximately 250 grid points.

The proposed model well predicts the experimental data for *1*-butanol and *iso*-butanol at 353 K from Princeton University [5]. The experimental data indicates that *iso*-butanol has a lower flame velocity than *1*-butanol, and this trend is reproduced by the model's predictions. The proposed model also well predicts the experimental data for all four isomers at 343 K from University of Southern California [3,4]. Both the experimental data and the model indicate that the flame velocities decreases as the degree of branching increases; *n*-butanol has the fastest flame velocity, *iso*-butanol and *sec*-butanol have similar flame velocities, and *tert*-butanol is the slowest (note changes is scale on the y-axis for the different isomers).

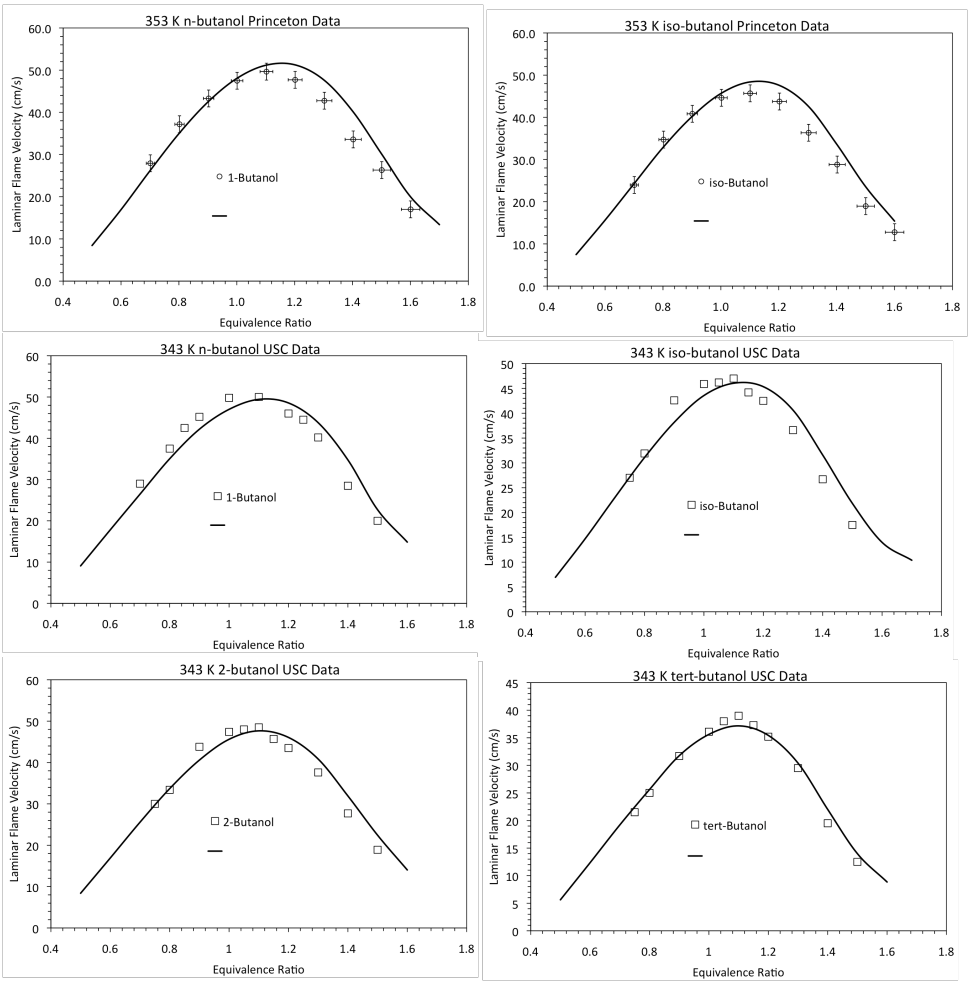

Figure 9 – Predicted and experimental premixed laminar flame velocity for the four butanol isomers. Experimental data is taken from Princeton [5] and USC [3,4].

3.5 Rapid Compression Machine Ignition Delay Simulations

The University of Connecticut has reported papid compression machine (RCM) ignition delay times for *1*-butanol, *iso*-butanol, and *tert*-butanol [7]. The RCM experimental data were obtained at ϕ=1 (in air), an end of compression pressure (Pc) of 15 atm, and end of

compression temperatures (Tc) on the range 725–855 K. The experiments were conducted at a compression time (tc) of 35 ms. The ignition delay time (τ_{id}) was defined as the time of maximum pressure rate rise (dP/dt) after the end of compression.

The present RCM simulations modeled the entire compression stroke using the initial pressure (Pi), intial temperatre (Ti), and compression time (tc), along with the volume history of a non-reactive pressure. Trace for heat loss mapping. The onset of ignition was determined as the point of maximum temperature rise (max dT/dt), which corresponds closely to the point of maximum pressure rate rise (max dP/dt). The simulated τ_{id} is plotted against the predicted Tc for each simulation run.

Figure 10 presents the experimental and predicted RCM ignition delay times. This study only presents predicted ignition delay times for *1*-butanol in the RCM. The experimental data indicates that *1*-butanol has shorter ignition delay times than the other three butanol isomers, which indicates enhanced low temperature reactivity. The proposed model well predicts the experimental data for *1*-butanol across the entire temperature range. At low temperatures, reactions of alphahydroxybutyl + O_2 are active, in addition to typical low temperature peroxy chemistry.

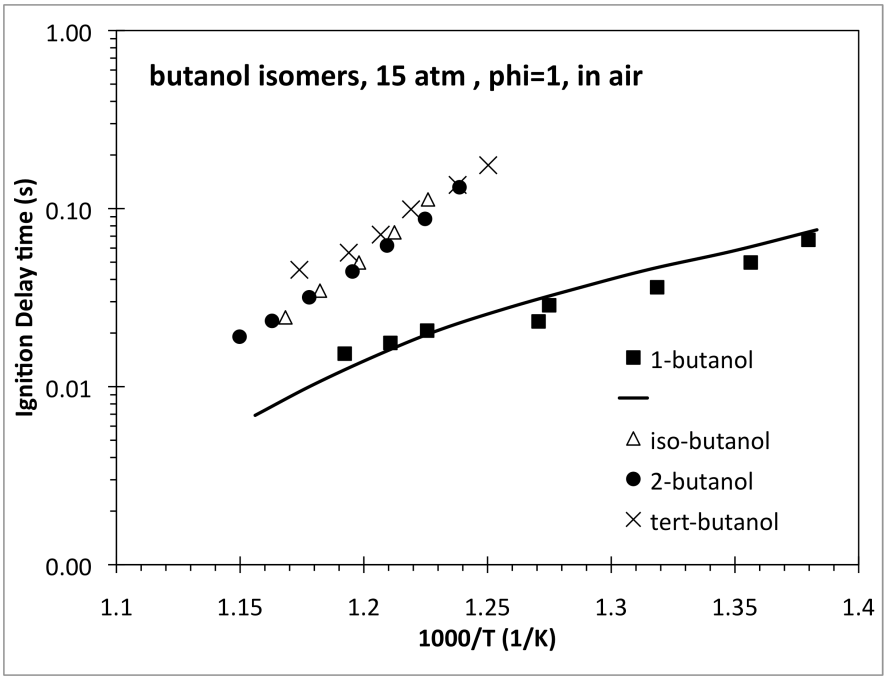

Figure 10 – RCM ignition delay times for butanol isomers from U. Conn. [7] and predicted values for *1*-butanol.

3.5 Shock Tube Ignition Delay Simulations

RWTH Aachen University has reported shock tube (ST) ignition delay times *1*-butanol in air (ϕ=1), a range of pressures from 10 bar to 80 bar, in the temperature range 770–1250 K [8,9]. The proposed model was validated against the experimental data by running constant volume homogeneous batch reactor simulations. The onset of ignition was determined as the point of maximum temperature rise (max dT/dt), which corresponds closely to the point of maximum pressure rate rise (max dP/dt).

Figure presents the experimental and predicted ST ignition delay times. The experimental data indicates that *1*-butanol ignition delay times decrease with increasing pressure, which indicates a direct relationship between fuel reactivity and pressure. Low temperature reactivity of *1*-butanol is observed at pressures above 20 bar. At all pressures, the proposed model well predicts the experimental data above 900 K. The experimental trend of increasing reactivity with pressure is also well reproduced by the model. The model over

predicts ignition delay times in the temperature range 795 – 900 K, which suggests that the model lacks low temperature reactivity.

Analysis of the proposed model indicates that low temperature reactivity is suppressed in the model due to the chosen reaction rate constant for the reaction alphahydroxybutyl + O_2 = nC_3H_7CHO + HO_2. This reaction is analogous to concerted elimination reactions in the low temperature oxidation of alkanes, which produce olefins and HO_2 and compete with low temperature chain branching reactions. We found that decreasing the rate constant of the aforementioned alphahydroxybutyl + O_2 reaction improved the low temperature ignition delay time predictions. However, we chose to keep the unmodified rate constant since it is based on the high pressure rate limit calculated by da Silva and Bozzelli [17] using a high level of theory.

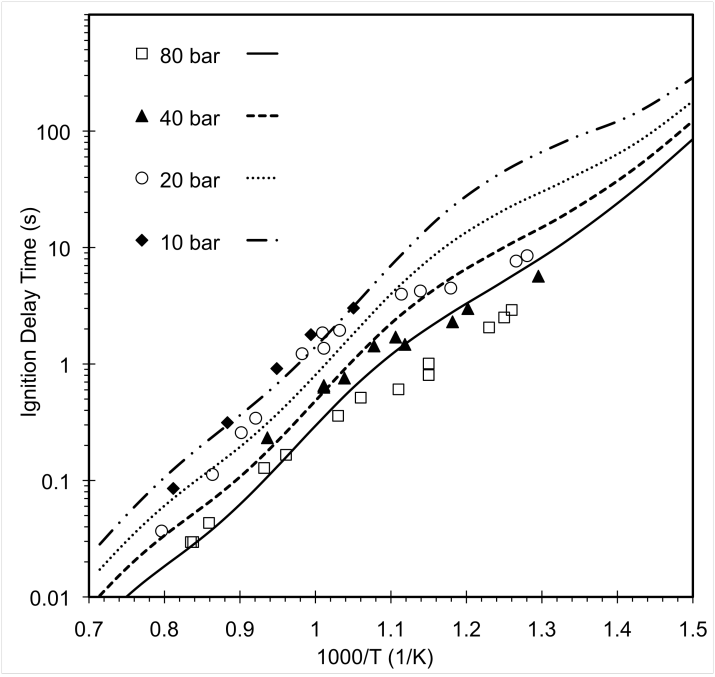

Figure 11 - Experimental [8,9] and predicted ST ignition delay times for for *1*-butanol.

4.0 Conclusions and Future Work

This paper presented a new model for the four isomers of butanol and compared it to experimental data from low-pressure premixed flames and premixed flame velocities. In the low-pressure premixed flames, the model indicates that H atom abstraction reactions are predominant and lead to the product species measured. Beta scission reactions are shown to be important at temperatures above 800 K; however, at regions of the flame nearer to the burner port, the lower temperatures and higher O_2 concentrations favor reactions of alphahydroxybutyl with O_2. These reactions were required to improve the prediction of C_4 aldehydes measured in the flames.

Enol-keto isomerizations assisted by HO_2 are also shown to be important in the low-pressure flames. True gas-phase tautomerizations and unimolecular dissociation reactions are negligible due to large energy barriers and the radical rich environment. Nevertheless, discrepancies for several aldehyde and ketone species may be due to surface catalyzed tautomerizations. Additional work is needed to improve the prediction of several highly unsaturated C3 and larger hydrocarbons. This can be accomplished by including reactions involving recombination of small unsaturated radicals to form larger unsaturated species.

The model also well reproduced the laminar flame velocity for all four butanol isomers; the general experimental trend of decreasing flame velocity with increasing structural branching is well reproduced by the model. *n*-Butanol RCM ignition delay times at 15 bar were well predicted by the model at both high and low temperatures. The model correctly reproduces high temperature ST ignition delay times, but it over predicts ignition delay times at temperatures below 900 K. The next step is to extend the model validation to low temperature conditions for all butanol isomers using data from rapid compression machines [7], high temperature shock tube ignition delay times [20], and

5.0 Acknowledgements

The portion of this work supported by LLNL Lawrence Livermore National Laboratory was performed under the auspices of the U.S. Department of Energy by Lawrence Livermore National Laboratory under Contract DE-AC52-07NA27344.

6.0 References

1. R. Grana, A. Frassoldati, T. Faravelli, U. Niemann, E. Ranzi, R. Seiser, R. Cattolica, K. Seshadri, Combust. Flame, Combustion and Flame 157 (2010) 2137–2154.
2. P. Oßwald, H. Güldenberg, K. Kohse-Höinghaus, B. Yang, T. Yuan, F. Qi, Combust. Flame 158 (2011) 2-15.
3. P.S. Veloo, F.N. Egolfopoulos, Proc. Combust. Inst. 33 (2011) 987-993.
4. P.S. Veloo, Y.L. Yang, F.N. Egolfopoulos, C.K. Westbrook, Combust. Flame 157 (2010) 1989–2004.
5. W. Liu, A.P. Kelley, C.K. Law, Proc. of the Combust. Inst. 33 (2011) 995–1002.
6. G. Black, H.J. Curran, S. Pichon, J.M. Simmie, V. Zhukov, Combust. Flame 157 (2) (2010) 363–373.
7. B. Weber, K. Kumar, C.-J. Sung. AIAA 2011-316, 49th AIAA Aerospace Sciences Meeting, (2011) Orlando, Florida.
8. K.A. Heufer, R.X. Fernandes, H. Olivier, J. Beeckmann, O. Roehls, N. Peters, Proc. Combust. Inst. (2010), doi:10.1016/j.proci.2010.06.052
9. S. Vranckx, K.A. Heufer, C. Lee, H. Olivier, L. Schill, W.A. Kopp, K. Leonhard, C.A. Taatjes, R.X. Fernandes, Submitted to Combust. Flame (2011).
10. C.-W. Zhou, H.J. Curran, J.M. Simmie, Combust. Flame (2010), doi:10.1016/j.combustflame.2010.11.002.
11. J.P. Orme, H.J. Curran, J.M. Simmie, J. Phys. Chem. A 110 (2006) 114–131.
12. H-.H Carstensen, A.M. Dean, in Computational Modeling in Lignocellulosic Biofuel Production, ACS Symposium Series, Vol. 1052 (2010), Chapter 10, 201–243.
13. G. da Silva, J.W. Bozzell, Chemical Physics Letters 483 (2009) 25–29.
14. C.K. Westbrook, W.J. Pitz, O. Herbinet, H.J. Curran, E.J. Silke, Combust. Flame 156 (2009) 181-199.
15. J. Zheng, D.G. Truhlar, Phys. Chem. Chem. Phys. 12 (2010) 7782–7793.
16. J.M. Simmie, H.J. Curran, J. Phys. Chem. A 2009, 113, 7834–7845
17. G. da Silva, J.W. Bozzell, J. Phys. Chem. A 2009, 113, 8923–8933 .
18. J.P. Senosiain, S.J. Klippenstein, J.A. Miller, J. Phys. Chem. A 2006, 110, 6960-6970.
19. U. Struckmeier, P. Oßwald, T. Kasper, L. Böhling, M. Heusing, M. Köhler, A. Brockhinke, K. Kohse-Höinghaus, Z. Phys. Chem. 223(4-5), 503–537, 2009 (contribution to special issue "Wagner Festschrift"), DOI: 10.1524.zpch.2009.6049
20. J.T. Moss, A.M. Berkowitz, M.A. Oehlschlaeger, J. Biet, V. Warth, P.-A. Glaude, F. Batti1-Leclerc, J. Phys. Chem. A 112 (43) (2008) 10843–10855.

7.0 Supplementary Material

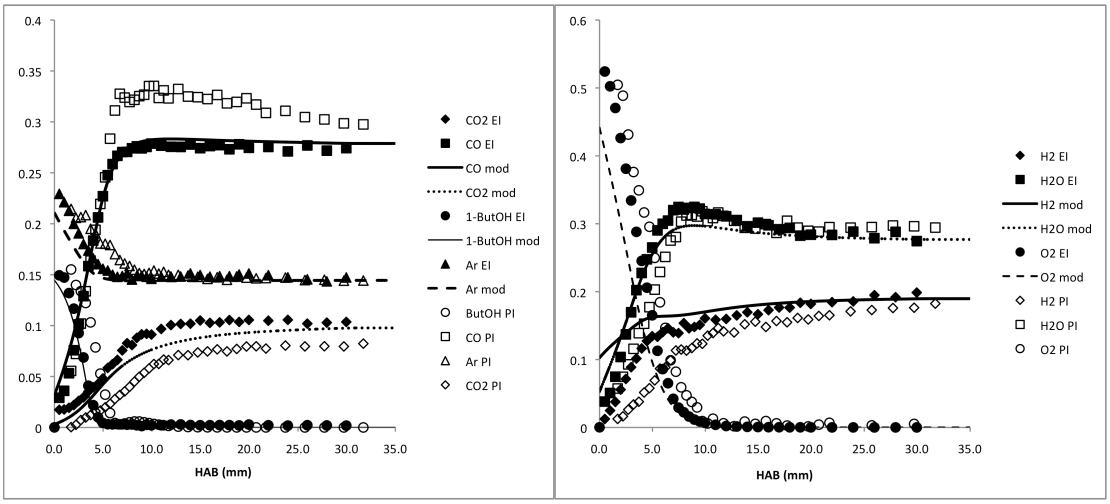

Figure 12 - Major species profiles for the *1*-butanol flame

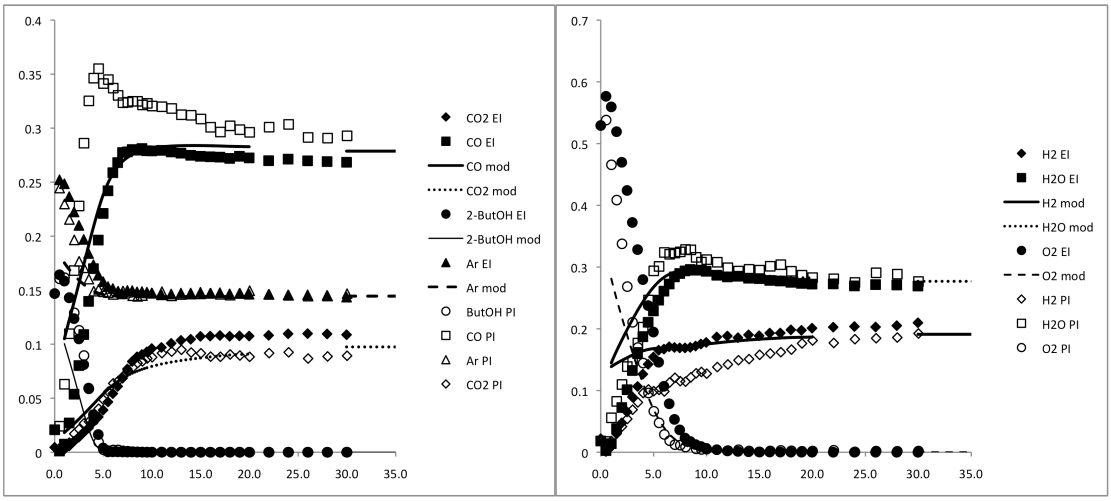

Figure 13 - Major species profiles for the *2*-butanol flame

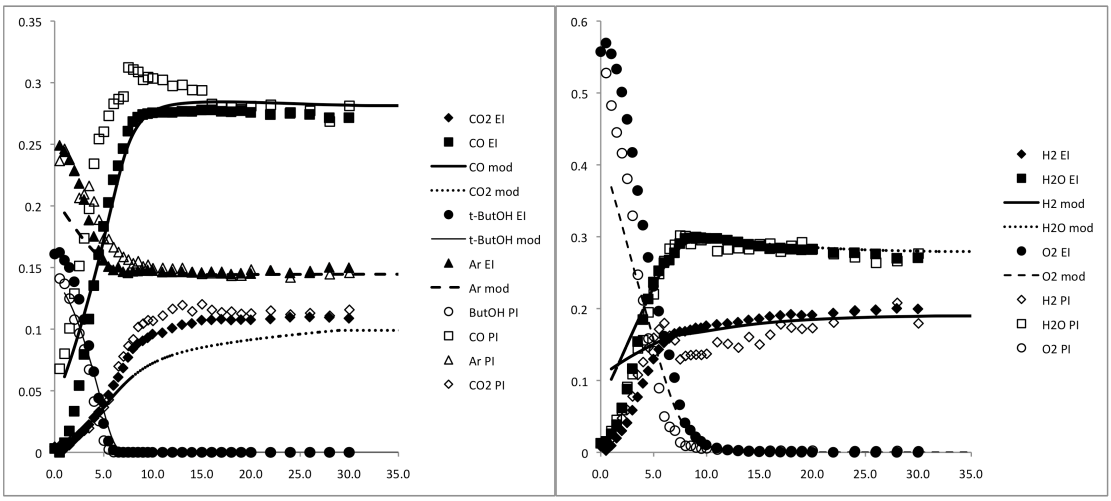

Figure 15 - Major species profiles for the *tertert*-butanol flame

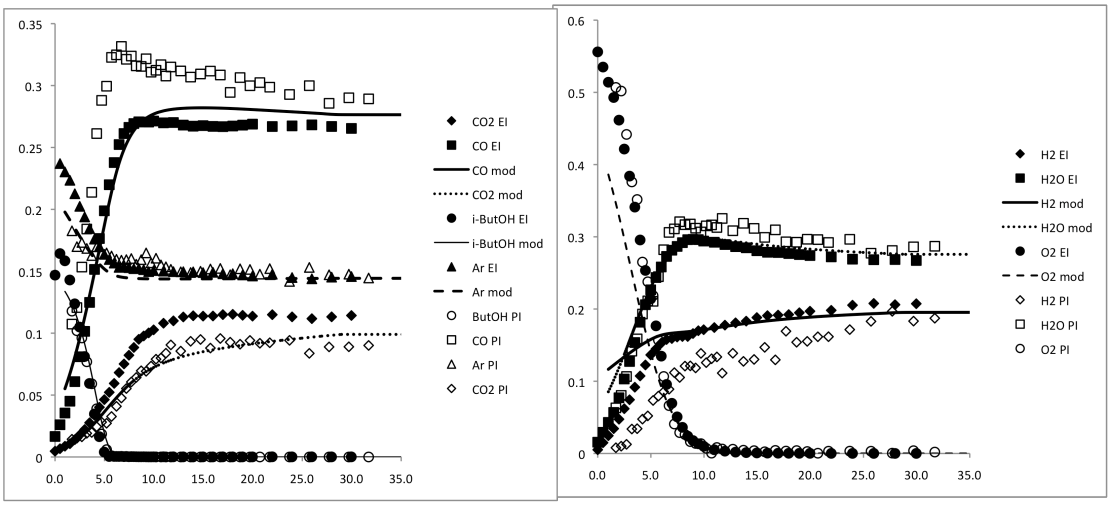

Figure 14 - Major species profiles for the *iso*-butanol flame